Revision 1

The single-crystal elastic properties of the jadeite-diopside solid solution and their implications for the composition dependent seismic properties of eclogite

MING HAO[1*], CAROLINE E. PIEROTTI[1,2], SERGEY TKACHEV[3], VITALI PRAKAPENKA[3], AND JIN S. ZHANG[1,4*]

[1]Department of Earth and Planetary Sciences, University of New Mexico, 221 Yale Blvd NE, Albuquerque, New Mexico 87131, U.S.A

[2]Albuquerque High School, 800 Odelia Rd NE, Albuquerque, New Mexico 87102, U.S.A

[3]GeoSoilEnviroCARS, University of Chicago, Argonne National Laboratory, Argonne, IL 60439, U.S.A

[4]Institute of Meteoritics, University of New Mexico, 221 Yale Blvd NE, Albuquerque, New Mexico 87131, U.S.A

*Corresponding authors: Ming Hao (minghao@unm.edu); Jin S. Zhang (jinzhang@unm.edu)

ABSTRACT

The 13 single-crystal adiabatic elastic moduli (C_{ij}) of a *C2/c* jadeite sample close to the ideal composition ($NaAlSi_2O_6$) and a natural *P2/n* diopside-rich omphacite sample have been measured at ambient condition by Brillouin spectroscopy. The obtained C_{ij}s for the jadeite sample are: C_{11} = 265.4(9) GPa, C_{22} = 247(1) GPa, C_{33} = 274(1) GPa, C_{44} = 85.8(7) GPa, C_{55} = 69.3(5) GPa, C_{66} = 93.0(7) GPa, C_{12} = 84(1) GPa, C_{13} = 66(1) GPa, C_{23} = 87(2) GPa, C_{15} = 5.4(7) GPa, C_{25} = 17(1) GPa, C_{35} = 28.7(6) GPa, C_{46} = 14.6(6) GPa. Voigt-Reuss-Hill averaging of the C_{ij}s yields

aggregate bulk modulus K_S = 138(3) GPa and shear modulus G=84(2) GPa for jadeite. Systematic analysis combing previous single-crystal elasticity measurements within the diopside-jadeite solid solution indicates that the linear trends are valid for most C_{ij}s. The Vp and Vs of omphacite decrease with Di content, though the velocity changes are small as Di component exceeds 70%. We also found that both the isotropic Vp and Vs as well as the seismic anisotropy of eclogite changed strongly with the bulk chemical composition. The relationship between the anisotropic velocities of eclogite and the chemical composition can be a useful tool to trace the origin of the eclogitic materials in the Earth's mantle.

Keyword: clinopyroxene, Brillouin spectroscopy, elastic properties, jadeite

INTRODUCTION

Clinopyroxene (Cpx) is one of the major mineral phases in the Earth's upper mantle (Ringwood 1975; Anderson and Bass 1984). The chemical composition of the upper mantle Cpx is close to Fe-bearing diopside (Di, $CaMgSi_2O_6$), with significant jadeite (Jd, $NaAlSi_2O_6$) component (e.g. Nestola et al. 2016). The crust of the subducted slabs and the delaminated lithosphere from continental roots form eclogite at depth >70-100 km (Irifune et al. 1986; Kay and Kay 1993). Cpx constitutes up to 70% of natural eclogite. The Cpx in eclogite is essentially Fe-bearing omphacite, which is the solid solution between Di and Jd. The coupled substitution of (Ca, Mg) for (Na, Al) in the Di-Jd solid solution stiffens the crystal structure, which has been confirmed by both the high-pressure single-crystal X-ray diffraction experiments and the sound velocity measurements (Pandolfo et al. 2012; Nestola et al. 2006; Sang et al. 2011; Kandelin and Weidner 1988; Zhang et al. 2016). The bulk (K_S) and shear (G) moduli of the end member Jd are ~25% and ~18% higher, respectively, than the end member Di (Sang et al. 2011; Kandelin and Weidner 1988).

In the Di-Jd solid solution, the chemical composition strongly influences the elastic properties and therefore, should be considered for modeling the seismic properties of pyrolite and eclogite.

The general chemical formula of Cpx is $(M2M1)Si_2O_6$. The M2 site is usually occupied by cations with larger ionic radii, such as Ca^{2+} and Na^{+}. The M1 site is slightly smaller, thus preferred by smaller cations, such as Mg^{2+} and Al^{3+}. At low-temperature conditions, the cations in the M1 and M2 sites are usually ordered, and the omphacite crystals show a lower *P2/n* symmetry, compared with the higher *C2/c* symmetry of the Di and Jd end members. As temperature increases, the ordering of the cations degrades in both the M1 and M2 sites, and eventually, the ordered *P2/n* structure will convert to a completely disordered *C2/c* structure at temperatures higher than ~725 ℃ (Fleet et al. 1978; Carpenter 1980).

Previous high-pressure equation of state studies in the Di-Jd solid solution (e.g. Pandolfo et al. 2012; Nestola et al. 2006; Zhang et al. 2016) provided constraints to the composition dependent isothermal bulk modulus (K_T). However, determination of the seismic velocities and elastic anisotropy requires direct single-crystal sound velocity measurements. The single-crystal elastic properties of Cpx with close to upper mantle chemical compositions have been studied previously (Levien et al. 1979; Sang et al. 2011; Collins and Brown 1998; Isaak and Ohno 2003; Bhagat et al. 1992; Walker 2012; Norris 2008; Skelton and Walker 2015). Levien et al. (1979) first measured the single-crystal elasticity of the Di end member using Brillouin spectroscopy, and the results were improved in a more recent study by Sang et al. (2011). Isaak and Ohno (2003) measured a Cr-bearing Di using resonant ultrasound spectroscopy, which agrees well with Sang et al. (2011), suggesting that the incorporation of small amounts of Cr has no resolvable effect on the elastic properties. A Cpx with more realistic and complicated upper mantle composition was measured by Collins and Brown (1998) using the stimulated light scattering technique. They found

some irregular trends that deviate from linear mixing models for C_{55}, C_{66}, and C_{35}. Omphacite has only once been measured at ambient condition by Bhagat et al. (1992). The sample used by Bhagat et al. (1992) is Jd-rich, whereas no single-crystal elasticity measurements are available for the Di-rich omphacites. Walker (2012) and Skelton and Walker (2015) theoretically calculated the C_{ij}s of Di, Jd, and $Di_{50}Jd_{50}$ at 0 K. They found that the linear mixing model did not work for C_{11}, C_{12}, C_{13}, and C_{23}. However, it remains unknown whether their conclusion still holds at temperatures higher than 0 K.

To improve our understanding of the single-crystal elastic properties of omphacite in the Di-Jd solid solution, we have measured the elastic properties of a *C2/c* Jd and a *P2/n* Di-rich omphacite at ambient condition. The accuracy and precision of the single-crystal Brillouin spectroscopy measurements are much better compared to several decades ago (Zhang et al. 2011; Bass and Zhang 2015). Employing the new results obtained in this study, we reanalyzed the elastic properties of the Di-Jd solid solution and explored the compositional effects on the seismic properties of eclogite over a wide compositional range.

EXPERIMENTAL METHODS

The compositions of the natural Jd and omphacite samples were measured by electron probe microanalysis (EPMA), using the JEOL 8200 Electron Microprobe facility hosted by the Institute of Meteoritics at University of New Mexico (UNM). Approximately 1 mm size crystals were polished and used for EPMA analysis, operating at 15 kV accelerating voltage and 20 nA beam current. The element standards were albite for Na, forsterite for Mg, almandine for Al and Fe, diopside for Si and Ca. Oxygen was calculated by stoichiometry from the cations. The detailed analysis results are summarized in Table 1. Normalizing the chemical analysis in terms of Di and Jd yields simplified compositions of $Di_{3.2}Jd_{96.8}$ for the Jd sample, $Di_{70.5}Jd_{29.5}$ for the omphacite

sample. The crystals were then double-side polished into pellets with ~15 μm thickness. They were scratch-free and inclusion-free under optical examination.

The unit-cell parameters and crystallographic orientations for all samples were determined by single-crystal X-ray diffraction at GeoSoilEnviroCARS experimental station 13-BM-D, Advanced Photon Source, Argonne National Laboratory. The X-ray was monochromated to 37.0 keV and focused to 3-4 μm × 7-8 μm. A stationary Perkin-Elmer image plate was used as the detector. Diffraction images were collected at 1°/step for the ±16° opening and the exposure time was 5 s/°. The obtained unit-cell parameters are: a = 9.439(5), b = 8.583(4), c = 5.228(1) Å, β = 107.50(2)°, and V_0 = 404.0(3) Å^3 (density ρ = 3.302(5) g/cm^3) for $Di_{3.2}Jd_{96.8}$; a = 9.632(3), b = 8.843(3), c = 5.245(1) Å, β = 106.31(2)°, and V_0 = 428.8(2) Å^3 (density ρ = 3.339(2) g/cm^3) for $Di_{70.5}Jd_{29.5}$. The space groups are also confirmed to be *C2/c* and *P2/n* for the Jd and omphacite sample, respectively.

For each sample, we used 3 different orientations for the single-crystal Brillouin spectroscopy measurements. The face normals of the measured samples are: (-0.692, 0.714, -0.106), (0.116, 0.993, -0.021), and (-0.043, 0.13, -0.999) for $Di_{3.2}Jd_{96.8}$; (-0.044, 0.979, 0.197), (0.242, 0.299, -0.923), and (0.697, 0.717, -0.016) for $Di_{70.5}Jd_{29.5}$. The accuracy of the measured plane normals is 0.5° or better.

The Brillouin spectroscopy experiments were performed in the high-pressure laser spectroscopy laboratory at UNM. We used a 300 mW 532 nm single-mode diode-pumped solid-state laser as the light source. The measurements were carried out using a 50° symmetric forward scattering geometry. The scattering angle was calibrated to be 50.37(5)° using a standard silica glass Corning 7980 (Zhang et al. 2011, 2015). For each crystal, shear velocities (*Vs*) and compressional velocities (*Vp*) were measured at 13 different χ angles (0, 30, 60, 90, 120, 150, 180,

195, 225, 255, 285, 315, 345) along the 360° azimuth to avoid any geometrical errors. All Brillouin spectra are with excellent signal-to-noise ratios. A typical Brillouin spectrum is shown on Figure 1.

RESULTS AND DISCUSSION

A least square inversion of the Christoffel equation was used to calculate the best-fit values for the 13-independent C_{ij}s at ambient condition (Weidner and Carleton 1977). The measured velocities associated with the velocity model predicted by the C_{ij} model of Jd are shown on Figure 2. The ambient K_S and G were calculated using the Voigt-Reuss-Hill (VRH) averaging scheme (Hill 1963). The K_S and G are 138(3) GPa and 84(2) GPa for $Di_{3.2}Jd_{96.8}$, and 123(3) GPa and 73(2) GPa for $Di_{70.5}Jd_{29.5}$, respectively.

Table 2 shows a complete list of the C_{ij}s obtained in this study alongside with both the results of the end member Jd measured by Kandelin and Weidner (1988), and those of the Jd-rich omphacite determined by Bhagat et al. (1992). The C_{ij}s of the $Di_{3.2}Jd_{96.8}$ sample measured in this study are in general agreement, yet with much smaller uncertainties, compared with Kandelin and Weidner (1988). The small amount of the Di component in our Jd sample may explain the smaller C_{12} and K_S determined in this study. As expected, most C_{ij}s of the $Di_{70.5}Jd_{29.5}$ sample measured in this study are smaller than the values of the $Di_{34.1}Jd_{65.9}$ omphacite measured by Bhagat et al. (1992).

Figure 3 shows the elastic moduli change as a function of chemical composition in the Di-Jd solid solution (Kandelin and Weidner 1988; Sang et al. 2011; Bhagat et al. 1992; Collins and Brown 1998; Isaak and Ohno 2003). We have utilized the following empirical polynomial function to describe the compositional dependence of the elastic moduli:

$$E = a_0 + a_1 * c + a_2 * c^2 \quad (1)$$

where E represents the elastic properties, including the C_{ij}s, K_S, and G; c is the proportion of the Di component in the Di-Jd solid solution; a_0, a_1, and a_2 are the fitting parameters shown in Table 3. The red shaded regions in Figure 3 represent the 95% confidence intervals. Similar to the negative correlation between the Di content and the K_T determined by previous X-ray diffraction experiments, the directly measured K_S and G linearly decrease with the Di content as well. Actually, all single-crystal elastic moduli show close-to-linear relationships with the Jd and Di content, except C_{13} and C_{23}. The C_{13} and C_{23} of omphacite are slightly higher and lower, respectively, than the predicted values from linear mixing models. The omphacite sample we measured is Cr-free. In Figure 3, most of the elastic moduli measured by Isaak and Ohno (2003) are actually within the shaded 95% confidence intervals. This confirms that a small amount of Cr does not have a noticeable influence on the elastic properties of Di as reported by Sang et al. (2011). It is also worth noting that the C_{33}, C_{55}, and C_{35} of the sample measured by Collins and Brown (1998) lie outside the trends determined from other measurements which may be explained by the high Tschermak's content (12mol%) of the sample measured by Collins and Brown (1998).

Skelton and Walker (2015) theoretically calculated the elastic properties of $Di_{50}Jd_{50}$ omphacite and compared with Walker (2012) to investigate the elasticity change within the Di-Jd solid solution at 0 K. They found out that the C_{11}, C_{12}, C_{13}, and C_{23} of omphacite were off from the linear mixing trend of Di and Jd. In this study, the C_{13} and C_{23} of omphacite are indeed slightly higher and lower than the values predicted by the linear mixing model. However, the C_{11} and C_{12} actually agree well (Figure 3). The difference between this study and Skelton and Walker (2015) may result from the temperature difference. Our measurements were carried out at room temperature whereas their calculation was performed at 0 K. Skelton and Walker (2015) suggested that the differential cation ordering between the M1 site and M2 site in omphacite caused the

158 nonlinear mixing. In particular, the cations in the M2 site are more disordered than M1 at low
159 temperatures. Elevating the temperature would disorder the cations within the crystal structure and
160 result in a close to linear mixing trend. This might explain the absence of the nonlinear mixing
161 trend in C_{11} and C_{12} observed in this study. The differences between the measured values and the
162 predicted linear mixing values of C_{13} and C_{23} are also smaller than what were calculated by Skelton
163 and Walker (2015). Further computational investigations at room-temperature condition can help
164 us quantitatively understand the differences between this experimental study and previous
165 theoretical investigations, as well as critically evaluate our explanations above.

166 **GEOPHYSICAL IMPLICATIONS**

167 Based on the measured single-crystal elastic properties, we calculated the aggregate *Vs* and
168 *Vp* within the Di-Jd solid solution (Figure 4a). Both the *Vp* and *Vs* display a nonlinear decrease
169 with the Di content. The composition induced velocity change is negligible as the Di component
170 exceeds 70%.

171 The Jd component of omphacite in natural eclogite varies from ~10% to ~65% (e.g.
172 Coleman et al. 1965; Bhagat et al. 1992; Smyth et al. 1991). Based on the compositional
173 dependence of the omphacite velocities obtained in this study, and the existing sound velocity
174 measurements of garnets (Sinogeikin and Bass 2002; Gwanmesia et al. 2014; Arimoto et al. 2015),
175 we calculated the *Vp* and *Vs* of 3 different eclogites at ambient condition assuming the Voigt
176 averaging scheme (Table 4, Coleman et al. 1965; Voigt 1889). The *Vp* and *Vs* of eclogite increase
177 with the Jd component in omphacite. In particular, the *Vp* and *Vs* differences between the eclogite
178 1 and 3 are as large as 3%. The bulk chemical composition of eclogite depends on its parent rock.
179 If the parent rock of eclogite has a strong continental and/or sediment component, the omphacite
180 in eclogite will be enriched in Na and Al, and thus high in Jd content (Irifune et al. 1994). The

relationship between the absolute velocities of eclogite and the chemical composition can be a useful tool to trace the origin of the eclogitic materials in the mantle.

Due to the elastically isotropic nature of the garnet, omphacite is the major anisotropy contributor in eclogite. Thus, in order to study the anisotropic seismic properties of eclogite, it is important to investigate the composition dependent elastic anisotropy in the Di-Jd solid solution.

In this study, universal anisotropy index (A^U), azimuthal *Vp* anisotropy (A^{Vp}) and radial *Vs* anisotropy (D^{Vs}) are calculated in the Di-Jd solid solution.

A^U is used as a measure of the overall elastic anisotropy for materials with arbitrary symmetry (Ranganathan and Ostoja-Starzewski 2008):

$$A^U = 5\frac{G^V}{G^R} + \frac{K_S{}^V}{K_S{}^R} - 6 \quad (2)$$

where the superscripts R and V refer to the Reuss and Voigt bounds of the homogeneous isotropic aggregate under VRH averaging scheme.

A^{Vp} represents the maximum velocity difference of all *Vp* propagating along different directions:

$$A^{Vp} = \frac{Vp_{max} - Vp_{min}}{Vp} \quad (3)$$

D^{Vs}, which describes the maximum velocity difference between the 2 orthogonally polarized shear waves propagating along the same direction, is defined as:

$$D^{Vs} = \frac{|Vs_1 - Vs_2|_{max}}{Vs}. \quad (4)$$

Figure 4b, 4c, and 4d show the anisotropy indices change as a function of chemical composition in the Di-Jd solid solution. The calculated anisotropy indices, especially the A^U and

A^{Vp}, of the Cpx sample measured by Collins and Brown (1998), lie outside the trends determined from all the other studies. This again may be explained by its high Tschermak's content (12mol%). The Di end member has the highest A^{U}, A^{Vp}, and A^{Vs} within the Di-Jd solid solution. The A^{Vp} decreases linearly as the Jd component increases. The A^{Vp} of the Di end member is 60% higher than that of the Jd end member. The trends in D^{Vs} and A^{U} are not as clear. Jd-rich omphacite seems to have similar D^{Vs} and A^{U} as Jd. Nevertheless, the enrichment of Jd component in omphacite is likely to decrease the overall elastic anisotropy of Cpx. The single-crystal elasticity data presented in this study can serve as the basis for future anisotropy modeling based on the lattice preferred orientation of the omphacite crystals in natural eclogite within a wide range of chemical compositions (Zhang et al., 2006; Zhang & Green, 2007).

ACKNOWLEDGMENT

The authors would like to thank Jane Silverstone (UNM), Jay Bass (UIUC) for providing the samples used in this study, Mike Spilde for the help with EPMA experiment at the Institute of Meteoritics at UNM. This work is supported by the National Science Foundation (NSF) under Grant EAR 1646527 (JZ) and the start-up fund from UNM (JZ). This research used resources of the APS, a U.S. DOE Office of Science User Facility operated for the DOE Office of Science by Argonne National Laboratory under Contract NO. DE-AC02-06CH11357.

REFERENCES CITED

Anderson, D.L. and Bass, J.D. (1984) Mineralogy and composition of the upper mantle. Geophysical Research Letters, 11, 637-40.

Arimoto, T., Gréaux, S., Irifune, T., Zhou, C., and Higo, Y. (2015) Sound velocities of $Fe_3Al_2Si_3O_{12}$ almandine up to 19 GPa and 1700 K. Physics of the Earth and Planetary Interiors, 246, 1-8.

Bass, J.D. and Zhang, J.S. (2015) Techniques for measuring high P/T elasticity. Schubert, Oxford.

Bhagat, S.S., Bass, J.D., and Smyth, J.R. (1992) Single-crystal elastic properties of omphacite-C2/c by Brillouin spectroscopy. Journal of Geophysical Research: Solid Earth, 97, 6843-6848.

Carpenter, M.A. (1980) Mechanisms of exsolution in sodic pyroxenes. Contributions to Mineralogy and Petrology, 71, 289-300.

Coleman, R.G., Lee, D.E., Beatty, L.B., and Brannock, W.W. (1965) Eclogites and eclogites: their differences and similarities. Geological Society of America Bulletin, 76, 483-508.

Collins, M.D. and Brown, J.M. (1998) Elasticity of an upper mantle clinopyroxene. Physics and Chemistry of Minerals, 26, 7–13.

Fleet, M.E., Herzberg, C.T., Bancroft, G.M., and Aldridge, L.P. (1978) Omphacite studies; I, The *P2/n* → *C2/c* transformation. American Mineralogist, 63, 1100-1106.

Gwanmesia, G.D., Wang, L., Heady, A., and Liebermann, R.C. (2014) Elasticity and sound velocities of polycrystalline grossular garnet ($Ca_3Al_2Si_3O_{12}$) at simultaneous high pressures and high temperatures. Physics of the Earth and Planetary Interiors, 228, 80-87.

238 Hill, R. (1963) Elastic properties of reinforced solids: some theoretical principles. Journal of the
239 Mechanics and Physics of Solids, 11, 357-372.

240 Irifune, T., Ringwood, A.E., and Hibberson, W.O. (1994) Subduction of continental crust and
241 terrigenous and pelagic sediments: an experimental study. Earth and Planetary Science
242 Letters, 126, 351-368.

243 Irifune, T., Sekine, T., Ringwood, A.E., and Hibberson, W.O. (1986) The eclogite-garnetite
244 transformation at high pressure and some geophysical implications. Earth and Planetary Science
245 Letters, 77, 245-256.

246 Isaak, D.G. and Ohno, I. (2003) Elastic constants of chrome-diopside: application of resonant
247 ultrasound spectroscopy to monoclinic single-crystals. Physics and Chemistry of Minerals, 30,
248 430–439.

249 Kandelin, J. and Weidner, D.J. (1988) The single-crystal elastic properties of jadeite. Physics of
250 the Earth and Planetary Interiors, 50, 251–260.

251 Kay, R.W. and Kay, S.M. (1993) Delamination and delamination
252 magmatism. Tectonophysics, 219, 177-189.

253 Levien, L., Weidner, D.J., and Prewitt, C.T. (1979) Elasticity of diopside. Physics and Chemistry
254 of Minerals, 4, 105-113.

255 Nestola, F., Ballaran, T.B., Liebske, C., Bruno, M., and Tribaudino, M. (2006) High-pressure
256 behaviour along the jadeite $NaAlSi_2O_6$–aegirine $NaFeSi_2O_6$ solid solution up to 10 GPa. Physics
257 and Chemistry of minerals, 33, 417-425.

Nestola, F., Alvaro, M., Casati, M.N., Wilhelm, H., Kleppe, A.K., Jephcoat, A.P., Domeneghetti, M.C., and Harris, J.W. (2016) Source assemblage types for cratonic diamonds from X-ray synchrotron diffraction. Lithos, 265, 334-338.

Norris, S. (2008) Elastic properties of jadeite. Undergraduate Senior Thesis. University of Illinois.

Pandolfo, F., Nestola, F., Cámara, F., and Domeneghetti, M.C. (2012) New thermoelastic parameters of natural *C2/c* omphacite. Physics and Chemistry of Minerals, 39, 295-304.

Ranganathan, S.I. and Ostoja-Starzewski, M. (2008) Universal elastic anisotropy index. Physical Review Letters, 101, 055504.

Ringwood, A.E. (1975) Composition and Petrology of the Earth's Mantle. McGraw-Hill, New York.

Sang, L., Vanpeteghem, C.B., Sinogeikin, S.V., and Bass, J.D. (2011) The elastic properties of diopside, $CaMgSi_2O_6$. American Mineralogist, 96, 224-227.

Sinogeikin, S.V. and Bass, J.D. (2002) Elasticity of Majorite and a Majorite-Pyrope solid solution to high pressure: Implications for the Transition Zone. Geophysical Research Letters, 29, 4-1.

Skelton, R. and Walker, A.M. (2015) The effect of cation order on the elasticity of omphacite from atomistic calculations. Physics and Chemistry of Minerals, 42, 677-691.

Smyth, J.R., Bell, D.R., and Rossman, G.R. (1991) Incorporation of hydroxyl in upper-mantle clinopyroxenes. Nature, 351, 732.

Voigt, W. (1889) Ueber die Beziehung zwischen den beiden Elasticitätsconstanten isotroper Körper. Annalen der physik, 274, 573-587.

278 Walker, A.M. (2012) The effect of pressure on the elastic properties and seismic anisotropy of
279 diopside and jadeite from atomic scale simulation. Physics of the Earth and Planetary
280 Interiors, 192, 81-89.

281 Weidner, D.J. and Carleton, H.R. (1977) Elasticity of coesite. Journal of Geophysical Research, 82,
282 1334-1346.

283 Zhang, D., Hu, Y., and Dera, P.K. (2016) Compressional behavior of omphacite to 47 GPa. Physics
284 and Chemistry of Minerals, 43, 707-715.

285 Zhang, J.S., Bass, J.D., and Zhu, G. (2015) Single-crystal Brillouin spectroscopy with CO_2 laser
286 heating and variable q. Review of Scientific Instruments, 86, 063905.

287 Zhang, J.S., Bass, J.D., Taniguchi, T., Goncharov, A. F., Chang, Y. Y., and Jacobsen, S. D. (2011)
288 Elasticity of cubic boron nitride under ambient conditions. Journal of Applied Physics, 109,
289 063521.

290 Zhang, J. and Green, H.W. (2007) Experimental investigation of eclogite rheology and its fabrics
291 at high temperature and pressure. Journal of Metamorphic Geology, 25, 97-115.

292 Zhang, J., Green II, H.W., and Bozhilov, K.N. (2006) Rheology of omphacite at high temperature
293 and pressure and significance of its lattice preferred orientations. Earth and Planetary Science
294 Letters, 246, 432-443.

Elements	$Di_{70.5}Jd_{29.5}$ (Wt%)	$Di_{3.2}Jd_{96.8}$ (Wt%)
Na_2O	4.13	14.65
MgO	11.77	0.42
Al_2O_3	7.59	24.42
SiO_2	54.73	59.62
CaO	17.59	0.81
FeO	3.59	0.69
Total	99.42	100.62

295 **Table 1.** The chemical composition of the Cpx samples used in this study.

	Jd		Omphacite	
ρ (g/cm^3)	3.302(5)	3.33	3.339(2)	3.327(2)
composition	$Di_{3.2}Jd_{96.8}$ This study	Jd Kandelin and Weidner (1988)	$Di_{70.5}Jd_{29.5}$ This study	$Di_{34.1}Jd_{65.9}$ Bhagat et al. (1992)
C_{11} (GPa)	265.4(9)	274(4)	231.7(8)	257(1)
C_{22} (GPa)	247(1)	253(4)	202(1)	216.2(8)
C_{33} (GPa)	274(1)	282(3)	255.2(9)	260.2(7)
C_{44} (GPa)	85.8(7)	88(2)	78.4(5)	80.2(6)
C_{55} (GPa)	69.3(5)	65(4)	68.9(5)	70.6(4)
C_{66} (GPa)	93.0(7)	94(2)	73.6(4)	85.8(5)
C_{12} (GPa)	85(1)	94(2)	85(1)	86(1)
C_{13} (GPa)	66(1)	71(8)	77(1)	76(1)
C_{23} (GPa)	87(2)	82(4)	58(2)	71(1)
C_{15} (GPa)	5.4(7)	4(3)	7.8(5)	7.1(6)
C_{25} (GPa)	17(1)	14(4)	6(1)	13(1)
C_{35} (GPa)	28.7(6)	28(3)	39.5(5)	33.7(8)
C_{46} (GPa)	14.6(6)	13(1)	6.3(4)	10.2(3)
K_S^R (GPa)	135.9(7)	141(2)	119.7(6)	128.0(5)
G^R (GPa)	82.7(3)	83(2)	72.0(3)	77.7(2)
K_S^V (GPa)	140.1(7)	145(2)	125.3(6)	133.5(5)
G^V (GPa)	86.3(3)	87(1)	75.5(3)	80.6(2)
K_S (GPa)	138(3)	143(2)	122(3)	130.8(5)
G (GPa)	84(2)	85(2)	74(2)	79.2(2)
V_p (km/s)	8.71(4)	8.77(5)	8.13(4)	8.43(4)
V_s (Km/s)	5.06(3)	5.05(5)	4.70(3)	4.88(3)
RMS error (m/s)	42.2	\	38.8	49

Table 2. Single-crystal elastic properties of different Cpx samples at ambient condition. The superscripts R and V refer to the Reuss and Voigt bounds of the homogeneous isotropic aggregate under VRH averaging scheme.

Elastic moduli	a_0	a_1	a_2
C_{11} (GPa)	267(4)	-39(4)	0
C_{22} (GPa)	243(4)	-64(4)	0
C_{33} (GPa)	273(6)	-33(7)	0
C_{44} (GPa)	84(1)	-5(2)	0
C_{55} (GPa)	71(2)	-2(2)	0
C_{66} (GPa)	89(4)	-12(4)	0
C_{12} (GPa)	89(2)	-10(3)	0
C_{13} (GPa)	64(3)	56(12)	-50(10)
C_{23} (GPa)	87(4)	-53(16)	26(13)
C_{15} (GPa)	5.3(7)	4.2(9)	0
C_{25} (GPa)	17(1)	-11(2)	0
C_{35} (GPa)	30(3)	12(4)	0
C_{46} (GPa)	12.8(9)	-6(1)	0
K_S (GPa)	139.7(8)	-26(1)	0
G (GPa)	83.1(9)	-12(1)	0

299 **Table 3.** The polynomial fitting results for the compositional dependence of the elastic moduli in

300 the Di-Jd solid solution. a_0, a_1 and a_2 are defined in Equation (1).

		Eclogite 1	Eclogite 2	Eclogite 3
Omphacite	Jd	10.5%	21.0%	45.5%
	Di	59.5%	49.0%	24.5%
Garnet	Pyrope	20.1%	13.5%	4.8%
	Grossular	3.6%	4.8%	6.9%
	Almandine	5.7%	11.7%	18.3%
Vs (km/s)		4.76	4.79	4.90
Vp (km/s)		8.26	8.36	8.51

Table 4. The end member mineral proportions, and calculated *Vp* and *Vs*, for the 3 eclogite samples.

We assume the volume proportion of omphacite and garnet are 70% and 30% for all 3 eclogites.

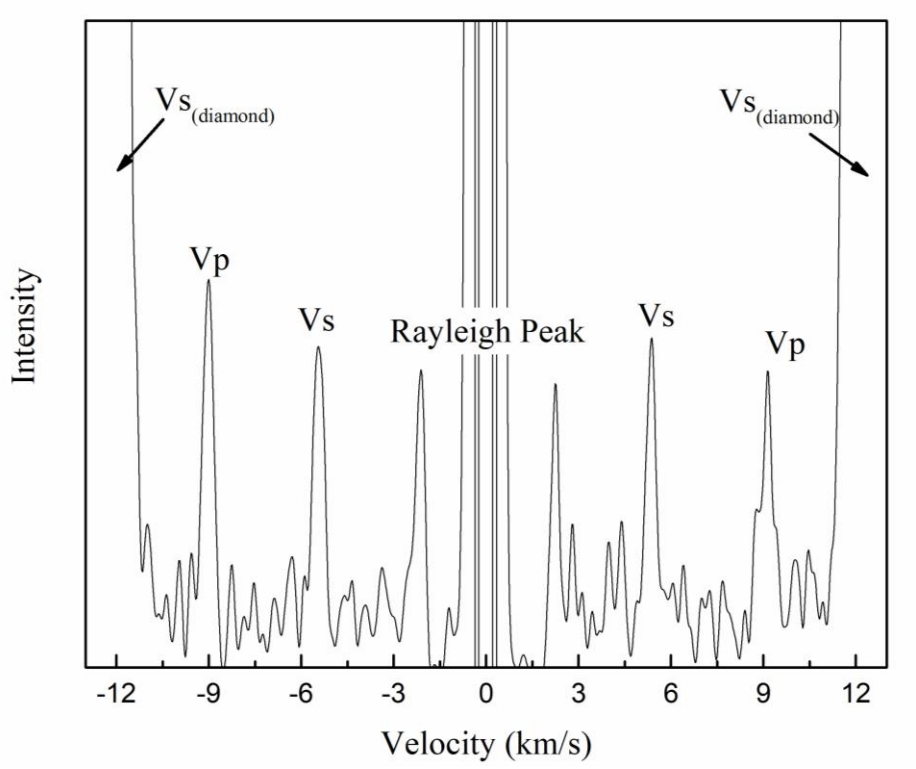

303

304 **Figure 1.** A typical the Brillouin spectrum showing one *Vs* and one *Vp* from the sample.

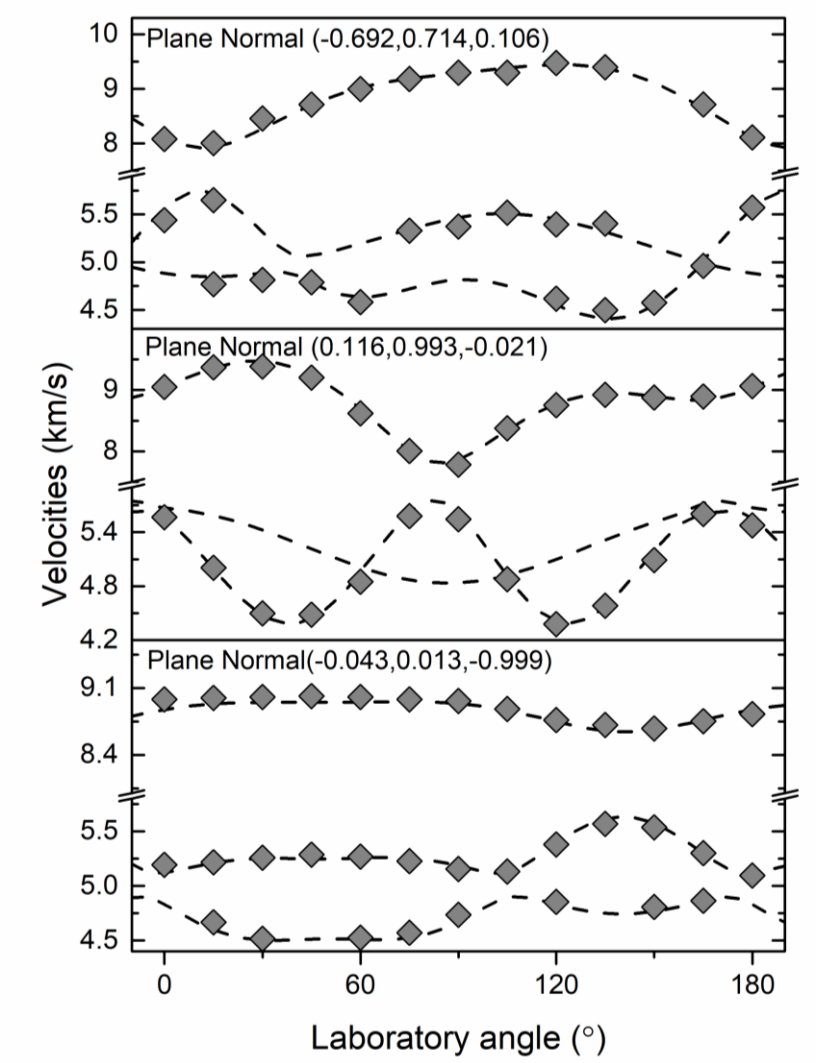

305

306 **Figure 2.** Measured acoustic velocities of Jd as a function of laboratory χ angles within the sample
307 plane. Dashed lines are the acoustic velocities calculated from the best-fit single-crystal elasticity
308 model; diamonds are the experimentally determined velocities. Errors are within the size of the
309 symbols.

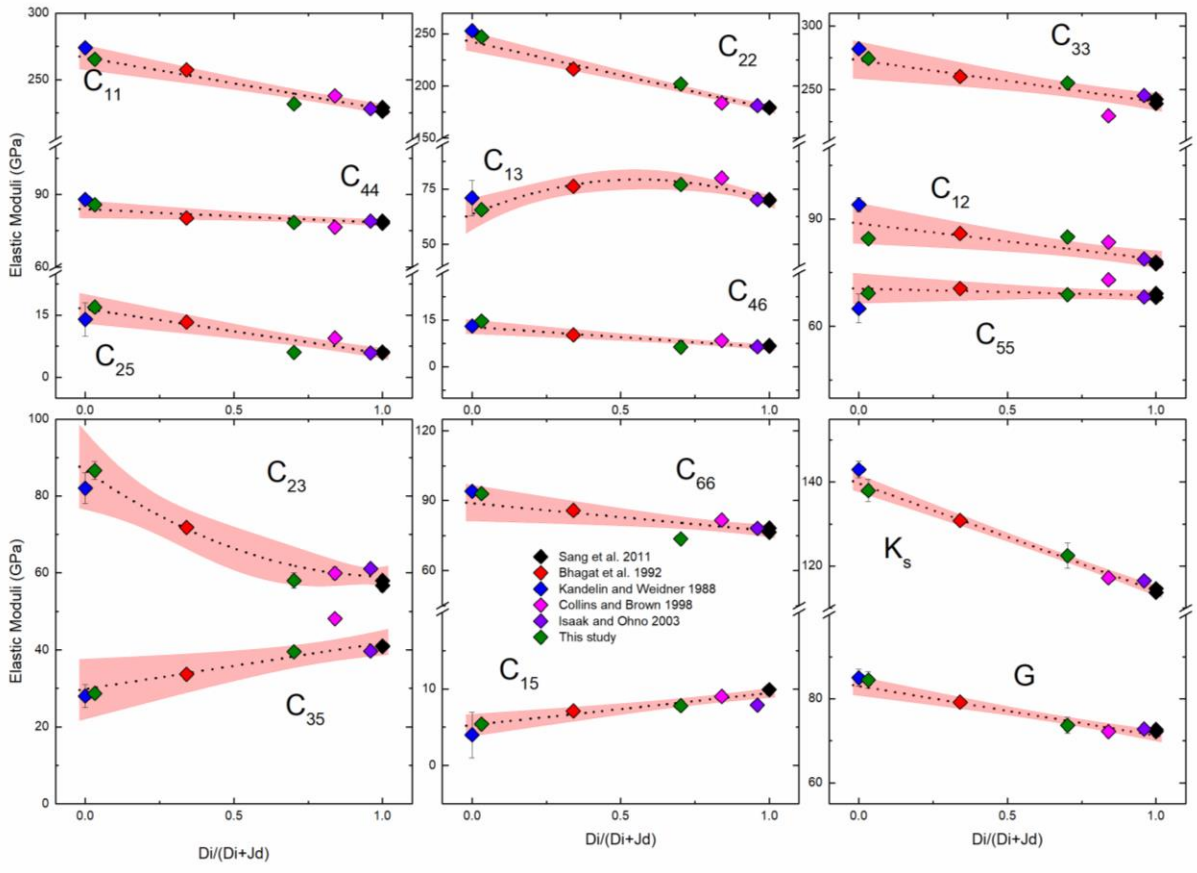

310

311 **Figure 3.** *C*ijs, *Ks*, and *G* as a function of chemical composition in the Di-Jd solid solution. The

312 red shaded regions represent the 95% confidence intervals.

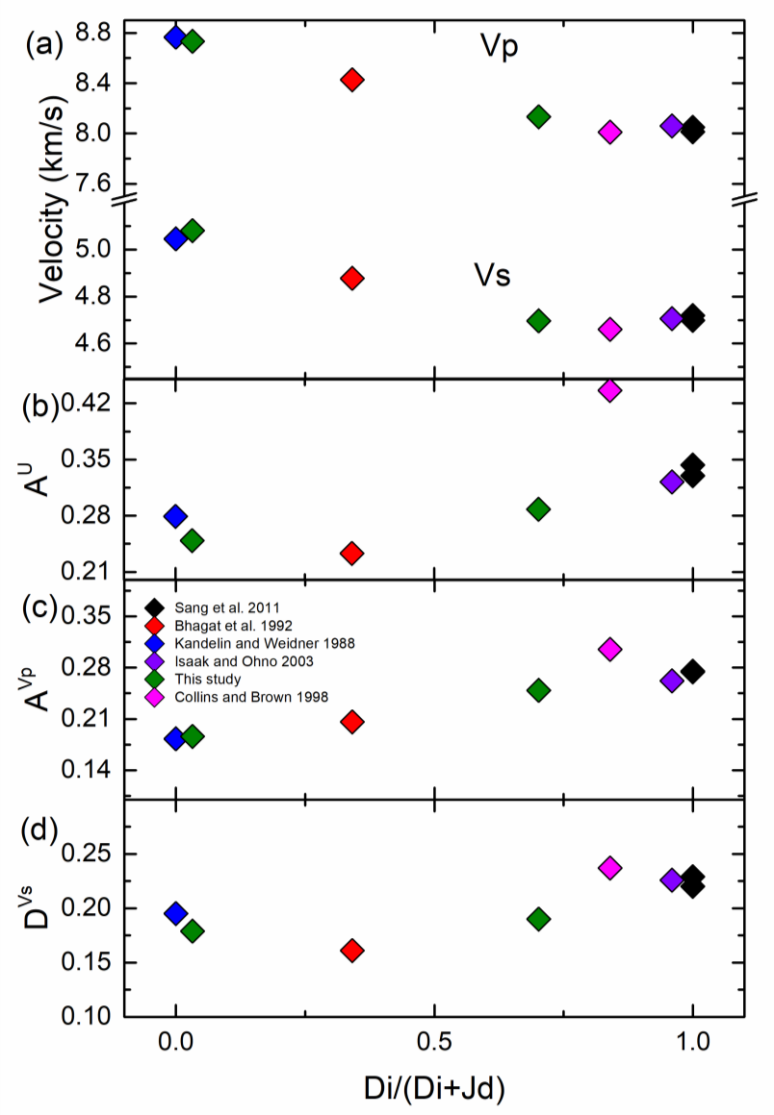

313

314 **Figure 4.** The velocities, A^U, A^{Vp}, and D^{Vs} as a function of chemical composition.